Water **2015**, *7*, 1480-1496; doi:10.3390/w7041480

OPEN ACCESS

water

ISSN 2073-4441
www.mdpi.com/journal/water

Article

Aluminum-Based Water Treatment Residue Reuse for Phosphorus Removal

Lai Yoke Lee *, Bibin Wang, Huiling Guo, Jiang Yong Hu and Say Leong Ong

Centre for Water Research, Department of Civil & Environmental Engineering, National University of Singapore, 1 Engineering Drive 2, 117576, Singapore; E-Mails: onebibin@gmail.com (B.W.) guohuiling@gmail.com (H.G.); ceehujy@nus.edu.sg (J.Y.H.); ceeongsl@nus.edu.sg (S.L.O.)

* Author to whom correspondence should be addressed; E-Mail: leelaiyoke@gmail.com; Tel.: +65-9320-4182.

Academic Editor: Maria Filomena Camões

Received: 16 January 2015 / Accepted: 27 March 2015 / Published: 1 April 2015

Abstract: Aluminum-based water treatment residue (Al-WTR) generated during the drinking water treatment process is a readily available recycled material with high phosphorus (P) adsorption capacity. The P adsorption capacity of Al-WTR generated from Singapore's water treatment plant was evaluated with reference to particle size range, adsorption pH and temperature. Column tests, with WTR amendments in sand with and without compost, were used to simulate the bioretention systems. The adsorption rate decreased with increasing WTR sizes. Highest P adsorption capacity, 15.57 mg PO_4^{3-}-P/g WTR, was achieved using fine WTR particles (>50% particles at less than 0.30 mm). At pH 4, the contact time required to reduce effluent P concentration to below the detectable range was half compared with pH 7 and 9. The adsorption rate observed at 40 ± 2 °C was 21% higher compared with that at 30 ± 2 °C. Soil mixes amended with 10% WTR and compost were able to maintain consistently high (90%) total phosphorus (TP) removal efficiency at a TP load up to 6.45 g/m^3. In contrast, TP removal efficiencies associated with columns without WTR amendment decreased to less than 45% as the TP load increased beyond 4.5 g/m^3. The results showed that WTR application is beneficial for enhanced TP removal in bioretention systems.

Keywords: phosphorus removal; water treatment residue; bioretention system; filtration media; secondary treated effluent

---

1. Introduction

Water treatment residue (WTR) generated from the addition of alum ($Al_2(SO_4)_3 \cdot 14H_2O$ or ferric chloride ($FeCl_3$) during the coagulation process in drinking water treatment offers a promising recycled material with high phosphorus (P) adsorption capacity. The use of WTR to control excess P in runoff as a result of fertilizer, manure or biosolids application in agricultural land has been receiving increasing attention [1,2]. More recent applications focus on the use of WTR in soil media of bioretention systems, more commonly known as rain gardens, to remove phosphate content from urban runoff [3]. In bioretention systems, plants only contribute to less than 20% of P retention, and therefore, WTR amendment could aid in long-term P removal [4]. Sandy media and loamy sand media, which are common mixes used in bioretention systems, would be exhausted in less than five years and a decade of stormwater loads, respectively [4,5]. In addition, the use of compost would result in significant performance deterioration due to exportation of P from compost [6]. However, compost constitutes an important organic source in the soil mix to sustain healthy plant growth and the soil microbial community. These are important elements in bioretention systems.

In Singapore, alum is mainly used in water treatment process for the removal of suspended matter. Aluminum-based WTR (Al-WTR) has been reported to have P adsorption capacities ranging from 6.6 to 18 g P/kg of WTR [1,7], while higher P adsorption of up to 23.9 g P/kg of WTR was attained at a lower reaction pH (pH 4) [8]. The P adsorption capacity of WTR is notably higher than other materials evaluated for P removal. These include red mud and Krazonem soil, which are native to Queensland, Australia and the U.S., respectively [3]. Likewise, the P adsorption capacities of perlite, zeolite and granular activated carbon (GAC) [9] are also lower than that of Al-WTR. Table 1 provides a summary on P adsorption capacities of the mentioned materials.

Table 1. Adsorbent materials for P removal.

Adsorbent	P Adsorption Capacity (g P/kg of Adsorbent)	References
Al-WTR	6.6–23.9	[1,7,8]
Red Mud	1.7	[3]
Krazonem soil	0.5	[3]
Perlite	0.01	[9]
Zeolite	0.13	[9]
GAC	1.16	[9]

Variations in P removal by WTR is a result of varying contents of aluminum oxide, other physicochemical parameters of the WTR, such as particle size, pH, retention time and the presence of inhibiting or competitive substances in the mixed liquor. Higher P adsorption values in WTR were also noted to correlate with higher aluminum oxides in the WTR. The general influences of the physicochemical parameters are summarized in Table 2.

The surface runoff characteristics in Singapore had been reported to be in the pH range of 6.3–8.1 with total phosphorus (TP) concentrations of 0.5–3.2 mg TP (as PO_4^{3-}-P)/L [10]; secondary treated effluents from conventional domestic wastewater treatment (using activated sludge process) were in the pH range of 6.5–7.5, with mean TP concentration of 4.1 mg TP/L [11,12]. In addition, runoff temperature could also vary significantly depending on the ambient temperature and temperature of the

surface with which runoff comes in contact [13]. These variations in pH, TP concentration and effect of runoff temperature could potentially influence Al-WTR performance for P adsorption. If Al-WTR were to be applied for P removal from runoff and/or secondary treated effluent, the P adsorption characteristics under these operating conditions would need to be determined. This paper therefore aims to evaluate the effects of WTR particle size, pH of reaction media and temperature on the P adsorption capacity and adsorption rate of the Al-WTR obtained from a local drinking water treatment plant. Column tests were further used to determine the P adsorption characteristics in mixes containing WTR and sand with or without compost.

Table 2. Influence of physicochemical characteristics on P adsorption by WTR.

Parameter	Influence	References
pH	Favors acidic conditions for P sorption due to hydroxyl competition and surface charge	[14,15]
Particle size	Increase P adsorption with decrease in particle size	[7]
Retention time	Longer retention time increases P adsorption, but generally achieved within 48 h	[7]
Synergistic/competitive substances	Calcium-synergistic	[16]
	Sulfate-competitive	[15,16]
	Nitrate-negligible	[17]

2. Materials and Methods

2.1. Water Treatment Residue

WTR from a local water treatment works in Singapore, which employs coagulation using alum (aluminum sulfate), was used in this study. The physicochemical characteristics of the filter-pressed WTR are given in Table 3. The filter-pressed WTR was dried at 50 °C over a 5-day period. Dried WTR was further crushed into smaller sizes and sieved for selection of particle size range prior to the experiments.

Table 3. Physicochemical characteristics of Al-WTR from a local water treatment works.

Physicochemical Properties	Value
Moisture content (%)	3.0
Organic matter (%)	12
Aluminum content (g/kg)	157.4
Analysis (g/kg)	-
Carbon	151.0
Hydrogen	45.2
Nitrogen	19.6
Sulphur	19.0

2.2. Experimental Phases

The experiment was carried out in three phases. Phase 1 (P1) was carried out in batch tests using shake flasks with synthetic water comprised of di-potassium hydrogen phosphate (K_2HPO_4) and

sodium chloride (NaCl) to simulate PO_4^{3-}-P and ionic strength, respectively. The WTR of four different particle size ranges was used to evaluate the PO_4^{3-}-P adsorption rates. In Phase 2 (P2), the effects of synthetic media pH and temperature on the PO_4^{3-}-P adsorption rate were studied using the optimum WTR size determined from Phase 1. Phase 3 (P3) was carried out to determine the performance of WTR in column tests by using the optimum WTR size (determined in Phase 1) blended at a 10% composition into different soil mixes.

2.2.1. Phase 1: PO_4^{3-}-P Adsorption Kinetics of Varying WTR Particle Size

The pre-dried WTR particles (at 50 °C) had average moisture and volatile solids content of 29.0% and 11.6%, respectively. After drying, the crushed particles were sieved through American Society for Testing and Materials (ASTM) sieves to obtain particle size ranges of more than 4.00 mm, 2.36–4.00 mm and 1.18–2.36 mm, while fine particles were obtained by further crushing the pre-dried particles of more than 4.00 mm using a pulverizer. Particle size distribution of the fine particles is summarized in Table 4. More than 50% of the fine particles was less than 0.30 mm.

Table 4. Particle size distribution of fine particles.

Particle Size (mm)	Portion (%)
>1.180	4
0.600–1.180	13
0.425–0.600	12
0.300–0.425	17
<0.300	54

Synthetic feed comprised of K_2HPO_4 (150 mg PO_4^{3-}-P/L) in 10.5 mg/L NaCl at pH ~7.2–7.3 was used to evaluate the effects of different WTR particle size ranges on P adsorption.

P1, Test 1: Adsorption Isotherms of Different WTR Particle Size Ranges

An amount of 150 mL synthetic feed was added into each 250-mL conical flask containing pre-weighed WTR of the respective particle size range and mixed using an orbital shaker (at 30 ± 2 °C, 200 rpm). The initial PO_4^{3-}-P concentration and concentration after 48 h were tested for each condition. Samples were filtered through 0.45-µm pore size filter paper (GN-6 Grid 47 mm, Gelman Science, Ann Arbor, MI, USA) prior to determination of PO_4^{3-}-P concentrations.

The Freundlich isotherm model has been commonly used to model adsorption of PO_4^{3-}-P onto solid adsorbents, such as aluminum oxide [17] and activated alumina [18]. Zhao *et al.* [19] further demonstrated this isotherm model as the best model to fit the equilibrium data of Al-WTR. The Freundlich isotherm is expressed in Equation (1):

$$\frac{x}{m} = K_f \text{ x } C_e^{1/n} \quad (1)$$

where: $\frac{x}{m} = \frac{(C_o - C_e)}{m}$ = mass of PO_4^{3-}-P absorbed per unit mass of WTR (mg PO_4^{3-}-P/g WTR). C_o = initial PO_4^{3-}-P concentration; C_e = equilibrium PO_4^{3-}-P concentration in the solution after

adsorption (mg PO_4^{3-}-P/L); m = mass of WTR used (g WTR); K_f = Freundlich capacity factor/maximum sorption capacity (mg PO_4^{3-}-P/g WTR); $1/n$ = Freundlich intensity parameter.

The Freundlich isotherm was used to model PO_4^{3-}-P adsorption on WTR in this study. Equation (2) is derived from Equation (1):

$$\log\frac{x}{m} = 1/n \log C_e + logK_f \quad (2)$$

The Freundlich capacity factor and intensity parameter can be determined by plotting $\log\frac{x}{m}$ against $\log C_e$ for the different particle size range.

P1, Test 2: Adsorption Rates of WTR with Different Particle Size Ranges

An amount of 150 mL synthetic feed was added into each 250-mL conical flasks containing 2.50 ± 0.05 g of WTR of different particle size ranges. Samples were collected and filtered through 0.45-µm pore size filter paper (GN-6 Grid 47 mm, Gelman Science, Ann Arbor, MI, USA). The filtrates were collected from each flask on an hourly basis for analyses of PO_4^{3-}-P concentrations. The absorption rate was then determined from the highest gradient on the slope of the plot with PO_4^{3-}-P concentration against contact time.

2.2.2. Phase 2: Effects of Reaction Media pH and Temperature on PO_4^{3-}-P Adsorption

Batch tests were carried out using 2.50 ± 0.05 g of fine WTR particles in 250-mL conical flasks containing 150 mL synthetic feed.

P2-Test 1: pH Effect

The reaction media were adjusted and maintained at pH 4.0 ± 0.5, 7.0 ± 0.5 and 9.0 ± 0.5 using 0.1 N hydrochloric acid (HCl). The adsorption tests were carried out in an incubator shaker (30 ± 2 °C, 200 rpm). Duplicate tests were performed for each condition, and samples were collected hourly.

P2-Test 2: Temperature Effect

The reaction media were buffered at pH 7.0 ± 0.5. The effect of temperature was evaluated at 30 ± 2 °C and 40 ± 2 °C in an incubator shaker set at 200 rpm. Duplicate tests were carried out for each condition, and samples were collected hourly.

Samples collected in this phase were filtered through 0.45-µm pore size filter paper (GN-6 Grid 47 mm, Gelman Science, Ann Arbor, MI, USA), and the filtrates were analyzed for PO_4^{3-}-P concentration. The maximum adsorption rate was determined as the highest rate of change in PO_4^{3-}-P concentration per unit time, and the specific adsorption rate was determined as the adsorption rate per unit mass of WTR used in the tests.

2.2.3. Phase 3: Phosphorus Removal Using 10% WTR Blended in Different Soil Mixes in Column Tests

Influent water characteristics: Secondary treated effluent from a local domestic wastewater treatment plant was used as the influent to the column to simulate polluted runoff. The domestic

wastewater treatment plant employed an anoxic-aerobic sequence that provided for enhanced nutrient removal. Hence, the total nitrogen (TN), TP, nitrate and phosphate (PO_4^{3-}) concentrations of the secondary treated effluent used in this study were significantly lower compared with conventional treatment plants that employed activated sludge process [11,12]. The quality of the secondary treated domestic sewage effluent is summarized in Table 5. The water quality of secondary treated effluent used in this study was found to be comparable to urban runoff. TP content was in the upper ranges of Singapore's urban runoff, as reported previously by Chui [10].

Table 5. Secondary treated domestic sewage effluent used in the study.

Parameters	Unit	Value (Average ± Standard Deviation)
pH	-	6.88 ± 0.30
Conductivity	μS/cm	681.29 ± 95.42
Turbidity	Nephelometric Turbidity Units (NTU)	2.49 ± 1.13
Total organic carbon (TOC)	mg/L	10.28 ± 0.58
TN	mg/L	3.01 ± 0.10
TP	mg/L	1.52 ± 0.12
PO_4^{3-}	mg/L	1.79 ± 0.15

The column tests were carried out using various soil mixes packed in clear acrylic columns of dimension 30 cm × 3.4 cm (height × internal diameter). The base of the column was packed with supporting gravels (particle size range of 10.0–22.0 mm) up to a height of 2 cm. This was followed by a 2-cm height of small gravels (particle size range of 1.5–3.0 cm) and a 20-cm height of soil mix as the filter media. This arrangement provided an effective empty bed volume of approximately 182 cm^3. Compositions of the four soil mixes used in this study are summarized in Table 6.

Table 6. Composition of soil mix in the column tests.

Column	Abbreviation	Composition
Column 1	C1	100% sand
Column 2	C2	90% sand and 10% WTR
Column 3	C3	85% sand, 10% WTR and 5% compost *
Column 4	C4	95% sand and 5% compost *

Note: * The compost used had moisture and organic matter contents of 19.5% and 51.5%, respectively.

A peristaltic pump was used to pump secondary treated effluent into the column from the top at a rate of 3 mL/min, equivalent to a hydraulic load of 0.2 m/h. The runoff was simulated in a batch sequence mode to represent each rainfall event. Each batch sequence was carried out by feeding 0.5 L secondary treated effluent and allowing it to percolate completely through the column before the effluent from each column was collected for water quality analysis. Feed and effluent samples were collected and analyzed for pH, TP and PO_4^{3-}-P concentrations. A schematic diagram of the column test set-up is shown in Figure 1.

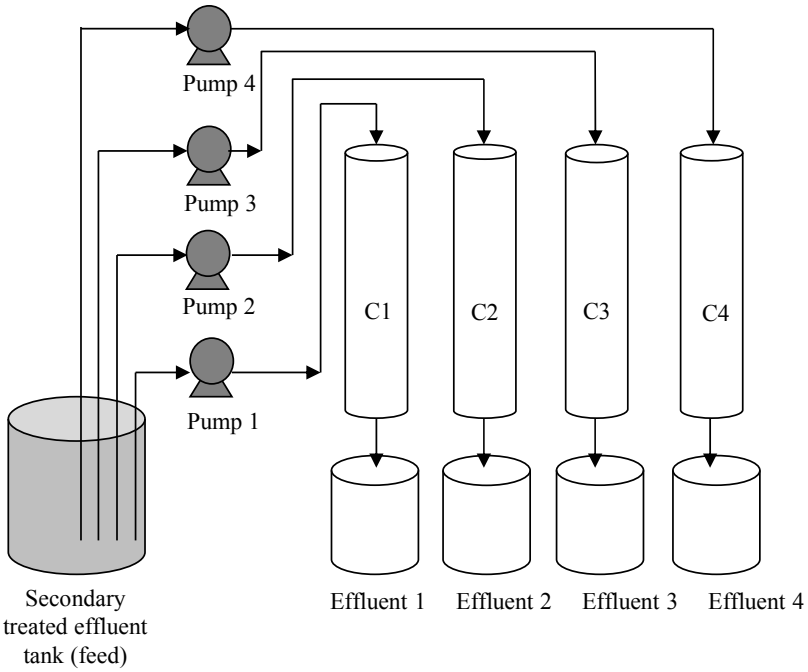

Figure 1. Schematic diagram of column test set-up using different soil mixes.

Treatment performance was evaluated against the bed volume of packing media and TP load (per unit packing media volume). TP load to the column is calculated based on Equation (3):

$$TP\ Load\ = \frac{C_{in}\ \cdot\ V_{in}}{V_{column}} \tag{3}$$

where TP load = total phosphorus load for every batch sequence (g/m^3); C_{in} = TP concentration in the feed for the particular batch sequence (g/m^3); V_{in} = feed volume of each batch sequence (m^3); V_{column} = volume of packing column (m^3).

Cumulative TP load for the n-th run is given by Equation (4):

$$\sum_{i=1}^{n} = TP\ load_{\,1} + TP\ load_{\,2} + \ldots\ldots\ldots + TP\ load_{\,n} \tag{4}$$

where $\sum_{i=1}^{n}$ = cumulative TP load for the *n*-th run (g/m^3) TP load$_1$ = TP load for batch Sequence 1 (g/m^3) TP load$_n$ = TP load for batch Sequence *n* (g/m^3).

2.2.4. Water Quality Analyses

pH was measured using the Horiba pH meter F-54 BW (Horiba Ltd, Kyoto, Japan), while TP was analyzed using PhosVer® 3 with the acid persulfate digestion method (Hach method 8190) [20]. PO_4^{3-} was analyzed using the Dionex LC 20 Chromatograph (Dionex Corporation, Sunnyvale, CA, USA) with a Dionex AS9-HC anion-exchange column after filtration using 0.45-µm pore size filter paper (GN-6 Grid 47 mm, Gelman Science, Ann Arbor, MI, USA). All water quality analyses were carried out in accordance with the Standard Methods for the Examination of Water and Wastewater Analysis [21].

3. Results and Discussion

3.1. Phase 1: P Adsorption Characteristics of WTR

Table 7 provides the *K* and *n* values determined from the experiments using Equation (2) after a 48-h contact time. The results demonstrated that the highest *K* value was obtained with fine WTR particles. The maximum PO_4^{3-}-P adsorption rate (15.57 mg PO_4^{3-}-P/g WTR) using fine WTR particles was comparable to the maximum adsorption capacities of Al-WTR reported by Dayton and Basta [7], which ranged from 6.6 to 16.5 g/kg after 17 h of equilibration. The *K* value obtained using WTR in this experiment was at least 4–6-times higher than that reported using aluminum oxide of a similar particle size range [17]. This could be due to the relatively higher Al content (157.9 g/kg) in the local WTR, which was about two-times more than that reported in other WTR materials [22]. Higher Al oxide content had been demonstrated to achieve higher PO_4^{3-}-P adsorption.

Intrapore specific surface area was also noted to be 24-times the average particle size [23]. Hence, smaller particles can significantly increase the intrapore specific surface area and, thus, higher effective area for PO_4^{3-}-P adsorption. This explains the significant increase in maximum PO_4^{3-}-P adsorption when the particle size was reduced from more than 1.18 mm to that of fine particles (with more than 50% of the particles being less than 0.30 mm).

Table 7. Freundlich isotherms *K* and *n* values for P adsorption by WTR with different particle size ranges.

Particle Size Range (mm)	*K*	*n*	R^2
Fine	15.57	6.41	0.9532
1.18–2.36	8.87	6.60	0.8428
2.36–4.00	4.72	7.15	0.9776
>4.00	3.05	7.34	0.8321

3.2. Effects of Particle Size on P Adsorption

The adsorption of PO_4^{3-}-P on Al-WTR was governed by the affinity of PO_4^{3-}-P onto active surface sites, such as through electrostatic interactions and ligand exchange reactions [24]. The adsorbed PO_4^{3-}-P could be bound directly on the oxide surface in accordance with the processes dictated in Equations (5) and (6) [9]:

$$Al_2O_3 + 3\ H_2O \leftrightarrow 2Al(OH)_3 \quad (5)$$

$$Al(OH)_3 + H_2PO_4^- \leftrightarrow AlPO_4 + OH^- + 2H_2O \quad (6)$$

Evidence showed that P adsorption onto Al_2O_3 was a mixture of complex mechanisms involving outer- and inner-sphere complexes with displacement of surface hydroxyl groups and water molecules with phosphate ions and surface precipitation [9,25].

Figure 2 illustrates the normalized residual PO_4^{3-}-P concentration in the reaction media corresponding to different contact time for the WTR particles of various size range. Within approximately 7 h, 2.5 g of fine WTR particles were able to remove the initial PO_4^{3-}-P concentration to a level below the detection limit. In contrast, the bigger WTR particles (1.18–4.00 mm) required approximately 24 h,

and those that were >4.00 mm required more than 24 h to achieve PO_4^{3-}-P levels below the detection limit. Thus, this study demonstrated the rate of PO_4^{3-}-P adsorption onto fine Al-WTR was rapid and the adsorption rate was strongly influenced by particle size (Figure 3). Fine particles also had the highest specific P adsorption rate, as compared with the bigger particles tested. The highest specific P adsorption rate of fine particles was observed to be 0.174 mg PO_4^{3-}-P/g WTR/min. This value was approximately two- and five- times the specific rates obtained with larger particle size ranges of 1.18–2.36 mm and >4.00 mm, respectively. The results indicated the adsorption was governed by intraparticle diffusion, which was highly significant in finer particles [18]. The diffusion of adsorbed PO_4^{3-}-P into the adsorbent resulted in precipitation of crystalline Al-phosphate and, eventually, irreversible binding of PO_4^{3-}-P onto the WTR particles [9,26].

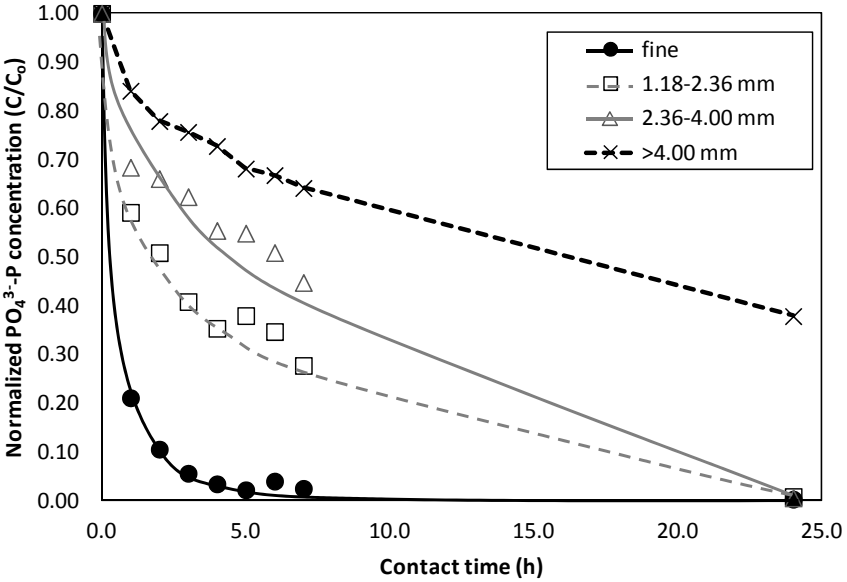

Figure 2. Normalized PO_4^{3-}-P concentration in the reaction media at different contact times.

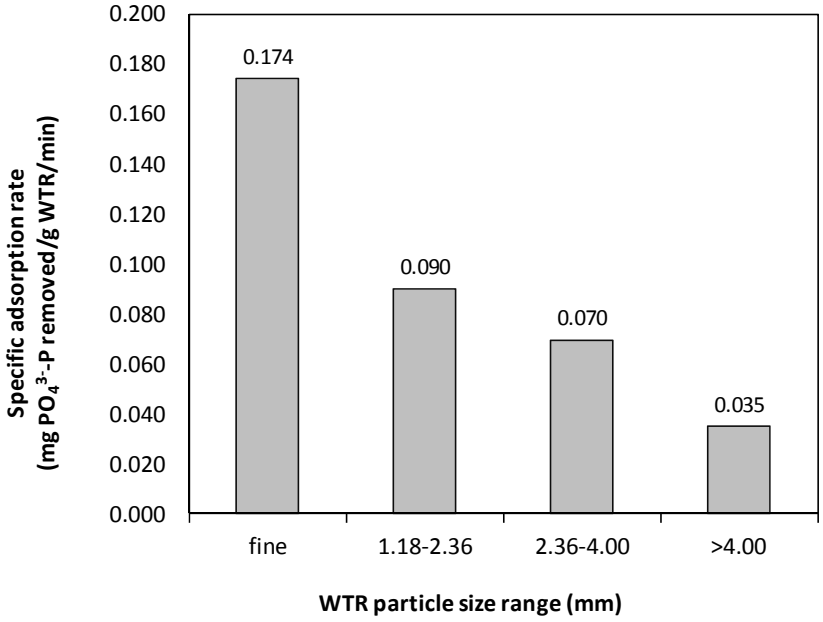

Figure 3. Effects of different particle size ranges on specific PO_4^{3-}-P adsorption rates of WTR.

It is important that rapid PO_4^{3-}-P adsorption is achieved during a rainfall event when stormwater infiltrates through a bioretention system. This is because the hydraulic flow varies considerably during each storm event depending on the rainfall intensity. In Singapore, the rainfall intensity could range from less than 10 mm/h to more than 50 mm/h [27]. Hence, this generates a high variation in the contact time as stormwater runoff flows through the filter media. The high adsorption capacity coupled with high adsorption rate using fine WTR particles could provide the characteristics required for PO_4^{3-}-P removal from stormwater runoff in bioretention systems.

3.3. Effect of pH on P Adsorption

Figure 4 shows the maximum specific PO_4^{3-}-P adsorption rate onto fine WTR particles was strongly dependent on pH of the synthetic feed. The specific PO_4^{3-}-P adsorption rate was observed to increase with a reduction in pH. The chemical sorption onto aluminum oxide media would result in an exchange with the hydroxyl group, leading to a subsequent increase in pH (Equation (6)). Hence, the reaction would favor slightly acidic reaction conditions [17,28].

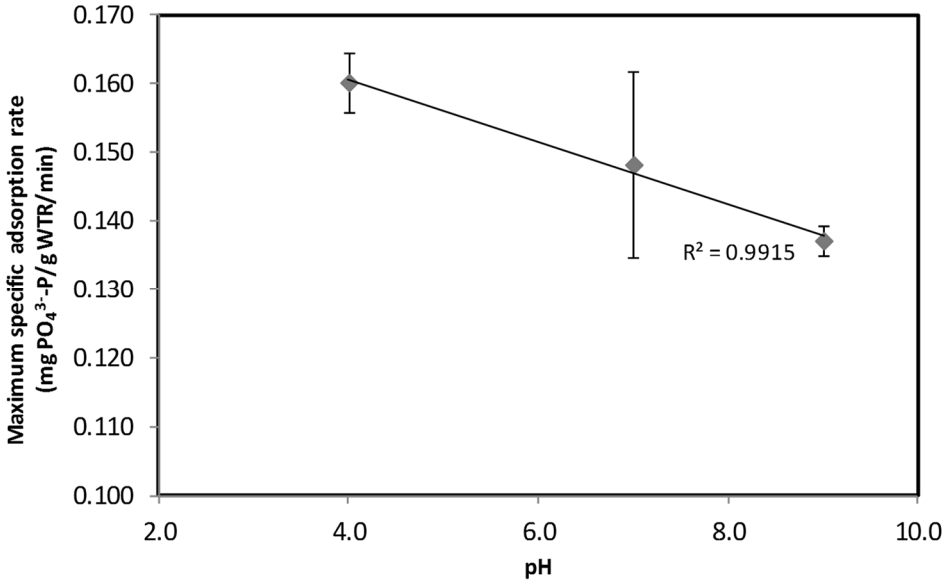

Figure 4. Maximum specific PO_4^{3-}-P adsorption rate at varying feed pH.

The P adsorption onto WTR observed in this study concurs with that reported for other aluminum oxide materials. It is observed that a higher PO_4^{3-}-P adsorption rate onto fine WTR was obtained at lower reaction media pH (pH 4) as compared with neutral conditions (pH 7). Conversely, the lowest PO_4^{3-}-P adsorption rate was obtained at pH 9. Yang *et al.* [15] demonstrated the change in zeta potential, which correlates with the WTR surface charge, from positive to negative as the reaction solution pH changed from acidic to alkaline condition. The increase in hydroxyl ions on the surface of WTR under alkaline condition would lead to a reduction in phosphate adsorption affinity. Thus, this reduced the adsorption rate as observed at pH 9 compared with that at a lower pH. Maximum sorption obtained at slightly acidic conditions (pH 5) was also reported with aluminum oxide media [15,17]. The P adsorption mechanisms onto WTR would be similar to that of alumina surfaces, which are related to ion exchange and complexation reactions [9,15,18]. Generally, the release of hydroxyl ions

leading to an increase in pH is expected when PO_4^{3-}-P is adsorbed onto WTR (as shown in Equation (6)). The maximum specific adsorption rate for WTR was noted at pH 4. This rate was at least 13% higher than that obtained at neutral pH. The subsequent increase in pH to pH 9 reduced the adsorption rate further to 0.136 mg PO_4^{3-}-P/g WTR/min.

The PO_4^{3-}-P removal efficiency at varying adsorption pH is shown in Figure 5. After 3 h of contact time, PO_4^{3-}-P removal of more than 90% was achieved at pH 4, while only 87% and 83% of PO_4^{3-}-P removal were achieved at pH 7 and 9, respectively. Overall, more than 48 h was required to reduce initial P concentrations to levels below the detectable limit at pH 7 and 9, while at the lower pH (pH 4), the contact time required for complete P adsorption was halved. However, extremely low pH may not be a favorable condition, as this would increase solubility and, hence, leaching of aluminum materials from the WTR [18]. The pH dependency is related to the amphoteric properties of WTR surface, which is similar to that reported on alumina and the polyprotic nature of phosphate [17].

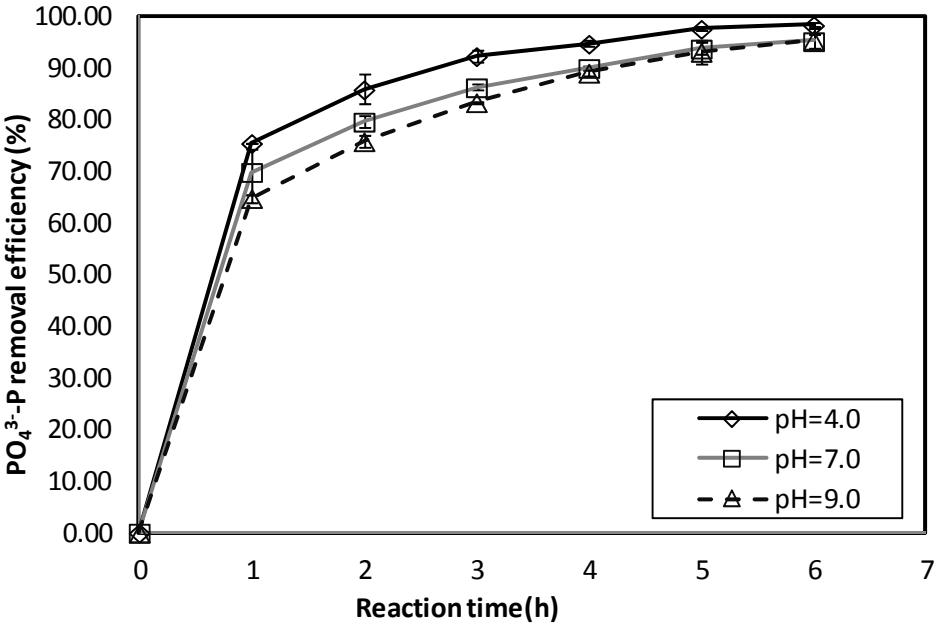

Figure 5. PO_4^{3-}-P removal efficiency at varying feed pH.

3.4. Effect of Temperature on P Adsorption

The results of PO_4^{3-}-P adsorption onto fine WTR particulates at different temperatures within the first 5 h of contact time are illustrated in Figure 6. This figure shows that PO_4^{3-}-P adsorption onto fine WTR particulates occurred at a high rate with maximum specific adsorption rate occurring within the first h. More than 60% of PO_4^{3-}-P removal was achieved at 30 ± 2 °C and 40 ± 2 °C within 1 h. Table 8 summarizes the maximum specific adsorption rates obtained at the two different temperatures. A higher PO_4^{3-}-P adsorption rate (about 21% more) was achieved at 40 ± 2 °C compared to that at 30 ± 2 °C during the first h. Zhang *et al.* [29] demonstrated that the P adsorption capacity of aluminum oxide was generally higher at a higher temperature. The *K* value in Zhang *et al.*'s [29] study was approximately 48% higher at 35 °C compared with 30 °C.

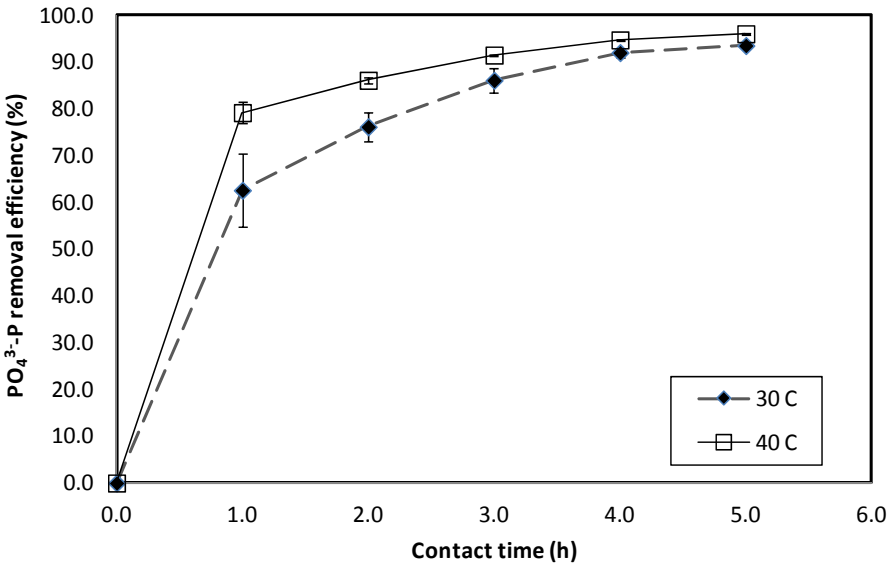

Figure 6. PO_4^{3-}-P removal using fine WTR particulates at varying temperature within the first 5 h of incubation.

Table 8. Maximum specific adsorption rate at different temperatures (within 1st hour of contact time) (n = 2).

Temperature (°C)	Adsorption Rate (mg PO_4^{3-}-P/g WTR/min)
30 ± 2	0.685 ± 0.084
40 ± 2	0.870 ± 0.021

At a contact time of 5 h, the PO_4^{3-}-P removal efficiency were 94% and 96% at 30 ± 2 °C and 40 ± 2 °C, respectively. After 24 h of contact time, close to 99% PO_4^{3-}-P removal efficiency was achieved at both temperatures. This observation demonstrated that a higher temperature promoted a more rapid P adsorption rate onto fine WTR particles. However, following prolonged contact time, the effect of temperature did not influence the final PO_4^{3-}-P removal efficiency. As the available adsorption sites and PO_4^{3-}-P concentration were similar for both conditions, similar P removal efficiency was achieved after more than 5 h of contact time.

The results from this study are important when applied to actual site conditions. The runoff temperature in tropical regions could vary in the range of 30–40 °C, depending on the surface temperature. On hot sunny days, heat may be transferred from hot impervious surfaces to the runoff, and hence, runoff that infiltrates into the soil mix would be of a higher temperature. Therefore, under such circumstances, the PO_4^{3-}-P adsorption onto WTR particles could occur at a higher adsorption rate as compared to times when runoff is at a lower temperature.

3.5. P Removal Using Soil Mixes in Column Tests

The potential of WTR for long-term P removal from a polluted water source was evaluated by mixing approximately 10% (based on weight) of WTR with soil mixes that are commonly used in bioretention systems, namely sand with or without compost [30]. Column 1 containing 100% sand was used as control.

TP in the simulated runoff would include particulate P, organic P and inorganic P (PO_4^{3-}-P). As noted in Figure 7, PO_4^{3-}-P removal efficiencies by the different soil mixes were mostly higher than TP removal efficiencies. This phenomenon could be attributed to the fact that WTR only adsorbed PO_4^{3-}-P. Particulate P and organic P, on the other hand, were not adsorbed by WTR. Particulate P could be trapped by the soil mix as it filters through the columns, while soluble organic P could remain in the treated runoff and flow out into receiving waterbodies. Similar results were observed in Lucas and Greenway's [3] study, where 97% PO_4^{3-}-P removal was reported as compared to only 93% removal of total dissolved P.

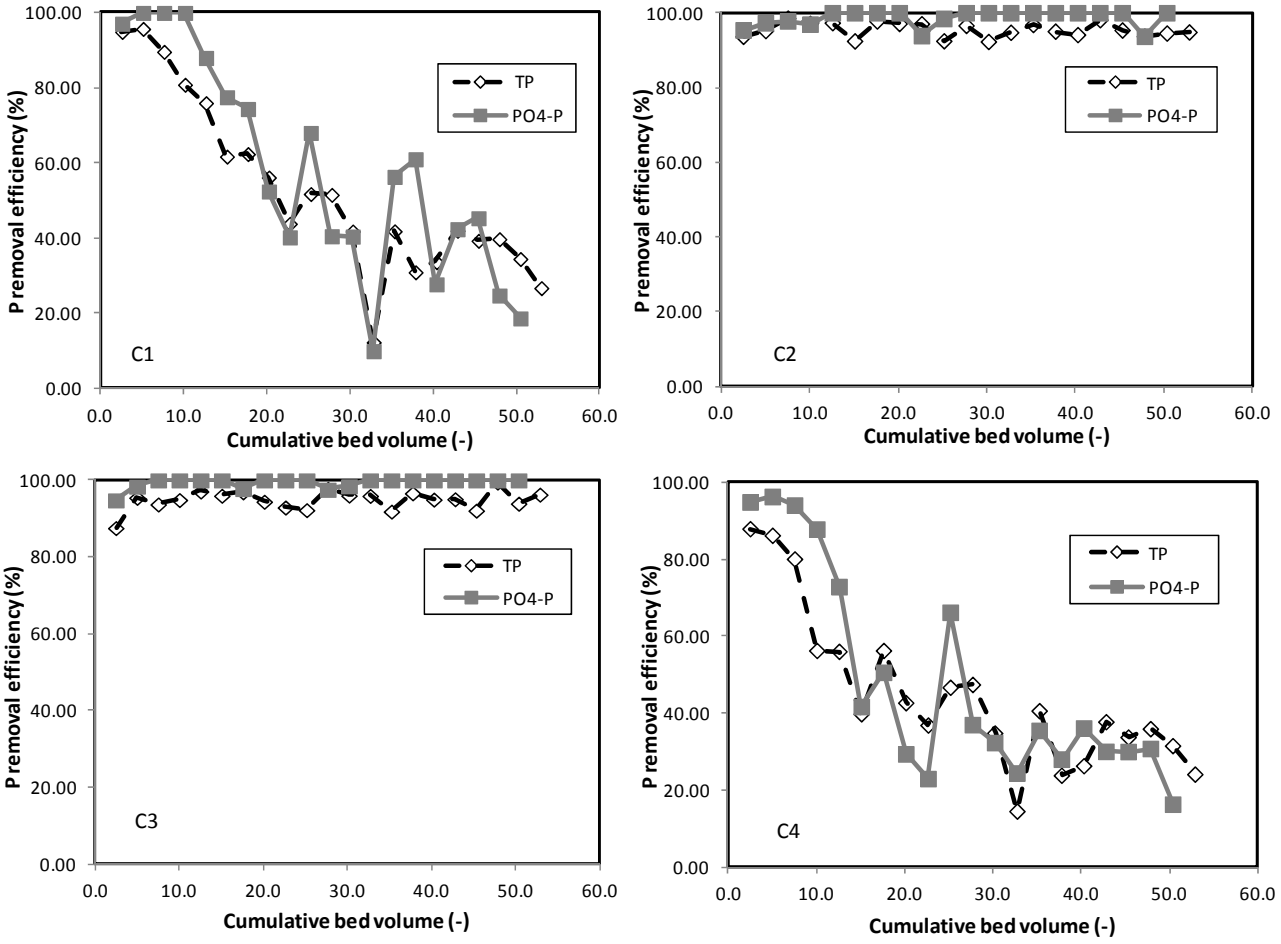

Figure 7. TP and PO_4^{3-}-P removal efficiency of different soil mixes; C1 contained 100% sand; C2 contained 90% sand + 10% WTR; C3 contained 85% sand + 10% WTR + 5% compost; C4 contained 95% sand + 5% compost.

The overall P removal from the simulated runoff using the different soil mixes was evaluated based on TP concentration. Figure 8 illustrates the cumulative TP load removal with respect to the TP load into the columns packed with different soil mixes used in this study.

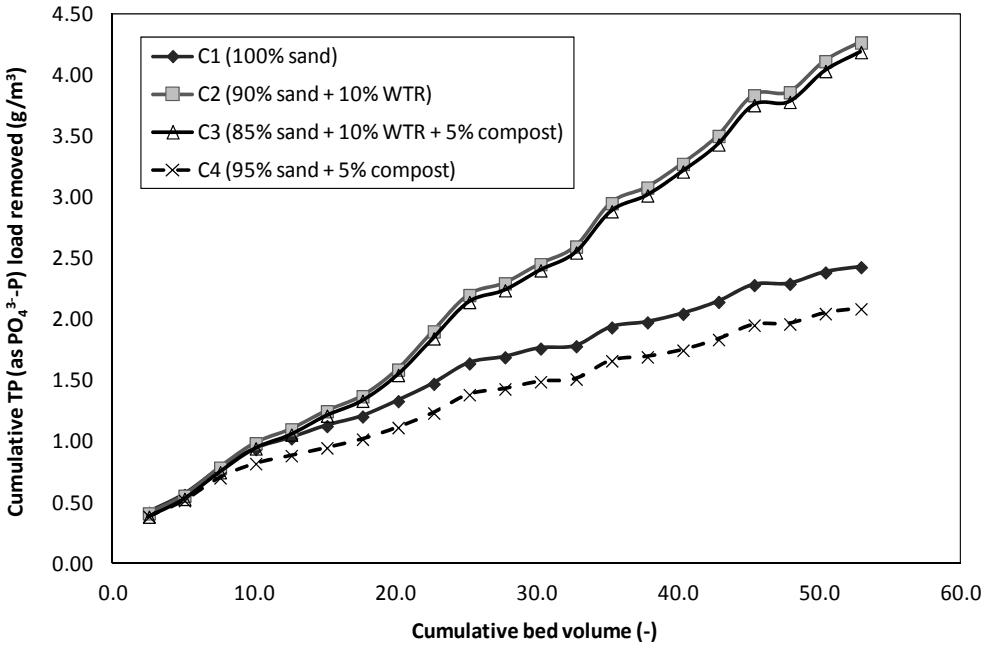

Figure 8. Cumulative TP load removed by different soil mixes.

It is noted from Figures 7 and 8 that the initial TP adsorption of all of the different soil mixes in the columns was insignificantly different up to a bed volume of 5.0 (or equivalent to 2.7 g TP/m^3) ($p > 0.05$, based on a two-sample *t*-test). Subsequently, as TP load increased, TP removal efficiencies by columns without WTR (Columns 1 and 4) decreased significantly from above 85% to below 45% when a TP load of more than 4.5 g TP/m^3 was applied (at more than a 30.0 bed volume). However, the columns containing 10% WTR (Columns 2 and 3) were able to maintain TP removal consistently above 90% throughout the study period. Table 9 summarizes the TP loads and removal efficiencies in columns containing 10% WTR.

Table 9. TP concentrations and removal efficiencies of columns containing 10% WTR.

Water Quality	Average ± Standard Deviation	
	Concentrations (mg TP as PO_4^{3-}-P/L)	Removal Efficiency (%)
Influent	1.52 ± 0.14	-
Effluent	-	-
Column 2 (90% sand + 10% WTR)	0.07 ± 0.03	95.5 ± 1.9
Column 3 (85% sand + 10% WTR + 5% compost)	0.08 ± 0.04	94.8 ± 2.6

Column 1 containing 100% sand demonstrated limited capacity in retaining TP. TP removal deteriorated sharply beyond a TP load of 3.01 g/m^3. This corresponded to bioretention studies that documented sandy media (at 85% sand by weight) could be exhausted after only five years' worth of TP loads from typical urban runoff [5].

The addition of 5% compost in sand media (Column 4) reduced the TP load removal by 14% as compared with the column containing only sand (Column 1). Column 4 was subjected to an overall

higher amount of P load due to the presence of compost, which has been known to leach P. Hence, it exhausted the sand's P adsorption capacity at a higher rate as compared to columns without compost (such as Column 1, which contained 100% sand). The addition of organic matter (10% compost and 10% mulch) to the soil media resulted in a net production of PO_4^{3-}-P in the column test reported by Bratieres *et al.* [6]. Similarly, in this study, the decrease in cumulative TP removal was observed in Column 4, which contained 5% compost after a cumulative TP load of more than 2.57 g/m^3 was fed to the column (corresponding to beyond a cumulative bed volume of about 7.6).

The results from this study demonstrated that columns containing 10% WTR were able to provide long-term TP removal. Even with 5% compost in the soil mix, the presence of 10% WTR maintained a high TP removal, and the cumulative TP load removal was insignificantly affected by P leaching from the compost ($p > 0.05$, based on a two-sample *t*-test). The cumulative TP loads removed in Columns 2 and 3 were at 4.27 and 4.19 g/m^3, respectively, when a TP load of up to 6.45 g/m^3 was applied to each column. The TP loads removed in these columns (Columns 2 and 3) were more than 2.0-times of those soil mixes without WTR. The column tests clearly demonstrated the ability of WTR to buffer TP removal capacity, even in the presence of materials that release P. Hence, WTR could provide a consistently low TP in the effluent (0.07–0.08 mg/L) to ensure high-quality treated water. Further, P adsorbed by Al-WTR has been reported to be irreversible and would remain stable for at least 7.5 years [1].

Although P adsorption onto aluminum oxide media has been reported to increase the treated water pH [17,18], such an observation was not evident in this study. The pH of the treated runoff was maintained at pH 6–8, which was within the acceptable pH range for discharge to receiving water bodies.

4. Conclusions

The high P adsorption capacity of recycled Al-WTR makes it highly attractive for application as a soil amendment for bioretention systems. In this study, the PO_4^{3-}-P adsorption capacities and adsorption rates were determined for locally obtained Al-WTR of various particle sizes. A high P adsorption rate and P adsorption capacity of 0.174 mg PO_4^{3-}-P/g WTR/min and 15.57 mg PO_4^{3-}-P/g WTR, respectively, were obtained for fine Al-WTR particles. This study also showed that the maximum specific PO_4^{3-}-P adsorption rate was highly dependent on adsorption pH, where the highest adsorption rate was observed at pH 4 as compared with pH 7 and pH 9. A temperature at 40 ± 2 °C provided a higher initial PO_4^{3-}-P adsorption rate (21% increase) as compared to 30 ± 2 °C, but both conditions resulted in close to 99% PO_4^{3-}-P removal efficiency following prolonged contact time (24 h). In column tests, soil mixes amended with 10% WTR were able to consistently sustain TP removal efficiencies of more than 95%, even in the presence of 5% compost, while TP removal efficiencies in soil mixes without WTR amendment deteriorated to about 45% when the TP load increased beyond 4.5 g TP/m^3. Hence, the use of Al-WTR amendment could sustain and lengthen the life-span of bioretention systems for TP removal.

Acknowledgments

The authors would like to thank the Public Utilities Board of Singapore for providing the water treatment residue used in this study.

Author Contributions

Lai Yoke Lee, Jiang Yong Hu and Say Leong Ong conceived of and designed the experiment. Jiang Yong Hu and Say Leong Ong contributed reagents, materials and analysis tools. Bibin Wang performed the experiment. Lai Yoke Lee, Bibin Wang, Huiling Guo analyzed the data and wrote the paper.

Conflicts of Interest

The authors declare no conflict of interest.

References

1. Agyin-Birikorang, S.; O'Connor, G.A. Lability of drinking-water treatment residuals (WTR) immobilized phosphorus: Aging and pH effects. *J. Environ. Qual*. **2007**, *36*, 1076–1085.
2. Babatunde, A.O.; Zhao, Y.Q. Constructive approaches towards water treatment works sludge management: An international review of beneficial re-uses. *Crit. Rev. Env. Sci. Technol.* **2007**, *37*, 129–164.
3. Lucas, W.C.; Greenway, M. Phosphorus retention by bioretention mesocosms using media formulated for phosphorus sorption: Response to acceletated loads. *J. Irrig. Drain. Eng.* **2011**, *137*, 144–152.
4. Lucas, W.C.; Greenway, M. Nutrient retention in vegetated and non-vegetated bioretention mesocosms. *J. Irrig. Drain. Eng.* **2008**, *134*, 613–623.
5. Hsieh, C.H.; Davis, A.P.; Needleman, B.A. Bioretention column studies of phosphorus removal from urban stormwater runoff. *Water Environ. Res.* **2007**, *79*, 177–184.
6. Bratieres, K.; Fletcher, T.D.; Deletic, A.; Zinger, Y. Nutrient and sediment removal by stormwater biofilters: A large-scale design optimization study. *Water Res.* **2008**, *42*, 3930–3940.
7. Dayton, E.A.; Basta, N.T. A method for determining the phosphorus sorption capacity and amorphous aluminium of aluminium-based drinking water residuals. *J. Environ. Qual.* **2005**, *34*, 1112–1118.
8. Yang, Y.; Zhao, Y.Q.; Kearney, P. Influence of ageing on the structure and phosphate adsorption capacity of dewatered alum sludge. *Chem. Eng. J.* **2008**, *145*, 276–284.
9. Ma, J.; Lenhart, J.H.; Tracy, K. Orthophosphate adsorption equilibrium and breakthrough on filtration media for storm-water runoff treatment. *J. Irrig. Drain. Eng.* **2011**, *137*, 244–250.
10. Chui, P.C. Characteristics of stormwater quality from two urban watersheds in Singapore. *Environ. Monit. Assess.* **1997**, *44*, 173–181.
11. Qin, J.J.; Oo, M.H.; Lee, H.; Kolkman, R. Dead-end ultrafiltration for pretreatment of RO in reclamation of municipal wastewater effluent. *J. Membr. Sci*. **2004**, *243*, 107–113.
12. Cao, Y.S. *Mass Flow and Energy Efficiency of Municipal Wastewater Treatment Plants*; IWA Publishing: London, UK, 2011.
13. Van Beuren, M.A.; Watt, W.E.; Marsalek, J.; Anderson, B.C. Thermal enhancement of stormwater runoff by pavement surfaces. *Water Res.* **2000**, *34*, 1359–1371.
14. Stumm, W.; Morgan, J.J. *Aquatic Chemistry: Chemical Equilibria and Rates in Natural Waters*, 3rd ed.; John Wiley and Sons: New York, NY, USA, 1996.

15. Yang, Y.; Zhao, Y.Q.; Babatunde, A.O.; Wang, L.; Ren, Y.X.; Han, Y. Characteristics and mechanisms of phosphate adsorption on dewatered alum sludge, *Sep. Purif. Technol.* **2006**, *51*, 193–200.
16. Rietra, R.; Hiemstra, T.; van Riemsdijk, W. Sulfate adsorption on goethite. *J. Colloid Interface Sci.* **1999**, *218*, 511–521.
17. Sansalone, J.J.; Ma, J.A. Parametric evaluation of batch equilibria for storm-water phosphorus adsorption on aluminum oxide media. *J. Environ. Eng.* **2009**, *135*, 737–746.
18. Brattebo, H.; Odegarrd, H. Phosphorus removal by granular activated alumina. *Water Res.* **1986**, *20*, 977–986.
19. Zhao, Y.Q.; Razali, M.; Babatunde, A.O.; Yang, Y.; Bruen, M. Reuse of aluminium-based water treatment sludge to immobilize a wide range of phosphorus contamination: Equilibrium study with different isotherm models. *Sep. Sci. Technol.* **2007**, *42*, 2705–2721.
20. Hach. Total-PhosVer® with acid persulfate digestion TNT method 8190. In *Water Analysis Handbook*, 5th ed.; Hach Company: Loveland, CO, USA, 2008.
21. American Public Health Association (APHA). *Standard Methods for the Examination of Water and Wastewater*, 20th ed.; American Water Works Association/Water Pollution Control Federation: Washington, DC, USA, 1998.
22. Ippolito, J.A.; Scheckel, K.G.; Barbarick, K.A. Selenium adsorption to aluminium-based water treatment residuals. *J. Colloid Interface Sci.* **2009**, *338*, 48–55.
23. Makris, K.C.; El-Shall, H.; Harri, W.G.; O'Connor, G.A.; Obreza, T.A. Intraparticle phosphorus diffusion in a drinking water treatment residual at room temperature. *J. Colloid Interface Sci*. **2004**, *277*, 417–423.
24. Stumm, W.; Kummert, R; Sigg, L. Ligand exchange model for the adsorption of inorganic and organic ligands at hydrous oxide interfaces. *Croat. Chem. Act.* **1980**, *53*, 291–312.
25. Bleam, W.F.; Pfeffer, P.E.; Goldberg, S.; Taylor, R.W.; Dudley, R. A phosphorus-31 solid-state nuclear magnetic resonance study of phosphate adsorption at the boehmite/aqueous solution interface. *Langmuir* **1991**, *7*, 1702–1712.
26. Tang, W.P.; Shima, O.; Ookubo, A.; Ooi, K. A kinetic study of phosphate adsorption by boehmite. *J. Pharm. Sci.* **1997**, *86*, 230–235.
27. National Environment Agency (NEA), Singapore. Singapore Weather, 2010. Available online: http://www.weather.gov.sg/online/loadNotesProcess.do (accessed on 30 March 2015).
28. Altundogan, H.S.; Tumen, F. Removal of phsophates from aqueous solutions by using bauxite. I: Effect of pH on the adsorption of various phosphates. *J. Chem. Technol. Biotechnol.* **2002**, *77*, 77–85.
29. Zhang, L.; Hong, S.; He, J.; Gan, F.; Ho, Y.S. Isotherm study of phosphorus uptake from aqueous solution using aluminium oxide. *Clean-Soil Air Water* **2010**, *38*, 831–836.
30. Facility for Advancing Water Biofiltration (FAWB). Advancing the Design of Stormwater Biofiltration, 2008. Available online: http://www.monash.edu.au/fawb/products/fawb-advancing-rain-gardens-workshop-booklet.pdf (accessed on 30 October 2014).